Research in Astron. Astrophys. **2013** Vol. **13** No. **12**, 1397–1408
http://www.raa-journal.org *http://www.iop.org/journals/raa*

Research in Astronomy and Astrophysics

Redshift drift reconstruction for some cosmological models from observations *

Ming-Jian Zhang and Wen-Biao Liu

Department of Physics, Institute of Theoretical Physics, Beijing Normal University, Beijing 100875, China; *wbliu@bnu.edu.cn*

Received 2013 May 27; accepted 2013 June 13

Abstract Redshift drift is a tool to directly probe the expansion history of the universe. Based on the Friedmann-Robertson-Walker framework, we reconstruct the velocity drift and deceleration factor for several cosmological models using observational $H(z)$ data from the differential ages of galaxies and baryon acoustic oscillation peaks, luminosity distance of Type Ia supernovae, cosmic microwave background shift parameter, and baryon acoustic oscillation distance parameter. They can, for the first time, provide an objective and quantifiable measure of the redshift drift. We find that reconstructed velocity drift with different peak values and corresponding redshifts can potentially provide a method to distinguish the quality of competing dark energy models at low redshifts. Better fitting between models and observational data indicate that current data are insufficient to distinguish the quality of these models. However, by comparing with the simulated velocity drift from Liske et al, we find that the Dvali-Gabadadze-Porrati model is inconsistent with the data at high redshift, which originally piqued the interest of researchers in the topic of redshift drift. Considering the deceleration factor, we are able to give a stable instantaneous estimation of a transition redshift of $z_{\rm t} \sim 0.7$ from joint constraints, which incorporates a more complete set of values than the previous study that used a single data set.

Key words: redshift drift: cosmology — reconstruction — observation

1 INTRODUCTION

The accelerating expansion of the universe is an extraordinary discovery in modern cosmology that followed Hubble's discovery of universal expansion. A number of independent cosmological probes over the past decade have supported this phenomenon. Examples include observations of Type Ia supernovae (SNeIa) (Riess et al. 1998), studies of large scale structure (Tegmark et al. 2004), and measurements of cosmic microwave background (CMB) anisotropy (Spergel et al. 2003). By contrast, Einstein's theory of general relativity suggests that there is a deceleration in the universal expansion caused by gravitational attraction from matter in the universe. Ironically, the cosmological constant, discarded by Einstein in his later years, is generally accepted as a theoretical explanation for this acceleration and has become a pillar of the modern standard cosmological model. In addition to the cosmological constant, there exist some other models that describe quite exotic

∗ Supported by the National Natural Science Foundation of China.

types of matter, such as quintessence (Peebles & Ratra 1988), K-essence (Armendariz-Picon et al. 2000), tachyon (Padmanabhan & Choudhury 2002), phantom (Caldwell et al. 2003), ghost condensate (Piazza & Tsujikawa 2004) and quintom (Feng et al. 2005). Regretfully, the origins of these dark energy variants so far have not been revealed within the standard model of (particle) physics. Instead of introducing a new mass-energy component, a number of new models try to explain the acceleration by replacing general relativity with a different theory of gravity, called modified gravity (see Nojiri & Odintsov 2007 for an introduction).

However, observations mentioned above are basically geometric in nature, because we usually extract the information on the expansion history from the angular diameter distance of the last scattering surface (CMB) and the luminosity distance (SNeIa), which require a prior on spatial curvature and hence a specific cosmological model (Liske et al. 2008b). Additionally, current probes are limited in terms of discriminating these dark energy models (Maor et al. 2001). In describing dark energy, an important parameter which links its pressure p and energy density ρ is the equation of state (EoS), $w(z) \equiv p(z)/\rho(z)$. For the most competitive candidate of dark energy, the cosmological constant, it gives $w = -1$. However, the latest Planck 2013 results (Planck Collaboration et al. 2013) show a deviation from –1. Moreover, the EoS can also be a function of redshift, such as in the Chevallier-Polarski-Linder (CPL) model. Hence, Maor et al. (2001) pointed out that a precise measurement of w today and its time variation $w' \equiv dw/dz|_{z=0}$ is appealing for distinguishing between the two possibilities and to provide important clues about the dynamical properties of dark energy. A direct and model-independent measure of the cosmic expansion history should clear up this confusion.

Sandage (1962) proposed a promising survey named redshift drift in order to directly probe the dynamics of the expansion. However, theoretical calculation indicates that it is difficult to detect because of its extremely weak magnitude. For example, the redshift drift Δz within an observational time interval of 10 yr for a source at this redshift coverage is of the order of only 10^{-9} in a standard ΛCDM model. The corresponding velocity drift Δv is also incompatible since it is only several cm s^{-1}. Fortunately, a possible scheme was later suggested from the wavelength shift of Lyα absorption lines in quasars (Loeb 1998). Nevertheless, continuous and extremely stable long term observations are required. The European Extremely Large Telescope (E-ELT) will be equipped with a high resolution, extremely stable, ultra high precision spectrograph named the COsmic Dynamics EXperiment (CODEX) that is designed to be able to measure such a small cosmic signal in the near future. Simulations that test the performance of this instrument have demonstrated its feasibility. Based on the power of CODEX, three sets of data (eight points) for the velocity drift were generated by Monte Carlo simulations of quasar absorption spectra with the assumption of a standard cosmological model (ΛCDM) (Liske et al. 2008a,b, 2009). Meanwhile, some other groups also produced similar data from this simulation method to study cosmological models. These corresponding data have been applied to constrain parameters in holographic dark energy (Zhang et al. 2007), modified gravity models (Jain & Jhingan 2010) and new agegraphic and Ricci dark energy models (Zhang et al. 2010), and found a better constraint on these models. In addition, Balbi & Quercellini (2007) investigated the redshift drift for a lot of dark energy models, and presented a valuable evaluation of them. An interesting aspect of the redshift drift not only comes from analyzing dark energy models, but also testing the Copernican Principle (Uzan et al. 2008). Recently, Darling (2012) showed a set of *observational* redshift drifts from the precise HI 21 cm absorption line by primarily using digital data from the Green Bank Telescope. This measurement lasted 13.5 yr for ten objects spanning redshift $z = 0.09 - 0.69$. Results listed in table 1 of Darling (2012) show that redshift drift is of the order of 10^{-8} yr^{-1}, which is about three orders of magnitude larger than the theoretical values. The author ascribes this discrepancy to the lack of knowledge on peculiar acceleration in absorption line systems and the long-term frequency stability of modern radio telescopes.

Although the available observations have some limitations, they also make a strong contribution to the analysis of dark energy, such as EoS (Wright 2007), the deceleration factor (Cunha 2009) and

so on. Therefore, the main purpose of this paper is to understand redshift drift using the available observational data.

This paper is organized as follows. In Section 2 the basic theoretical background of the redshift drift is introduced. The reconstruction method of the objective functions and relevant data are shown in Section 3. Reconstruction results for specific cosmological models are provided and discussed in Section 4. Our final conclusion and discussion are presented in Section 5.

2 THE REDSHIFT DRIFT

Redshift drift is the first method related to a direct measurement of the cosmic expansion history, which does not require any cosmological priors whatsoever. Previous observations, for instance the CMB, SNeIa, weak lensing and baryon acoustic oscillation (BAO), are essentially *geometric* in nature, or a prior on spatial curvature is assumed in advance. However, the most remarkable trait of a redshift drift experiment is its direct probe of the global *dynamics* of the metric, as described by Liske et al. (2008a). Although many targets like masers and molecular absorptions have been put forward, the most promising candidate rests in the Lyα forest in the spectra of high-redshift quasars (Pasquini et al. 2006). These are not only far away from the noise of the peculiar motions relative to the Hubble flow, but also possess the useful aspect of having a large number of lines in a single spectrum. Above all, the E-ELT, which will host CODEX, is designed to have the necessary photon collecting power to observe redshift drift by stably monitoring the redshifts of quasar absorption lines over a timescale of $\sim$20 yr. Fortunately, Pasquini et al. (2005) have checked that 25 quasars are presently known at redshift $z = 2 - 4$ with magnitude brighter than 16.5.

A signal emitted by a source at $t_{\rm em}$ can be observed at time t_0. Because of expansion of the universe, the source's redshift should be given through the scale factor

$$z(t_0) = \frac{a(t_0)}{a(t_{\rm em})} - 1\,. \tag{1}$$

Over the observer's time interval Δt_0, the source's redshift becomes

$$z(t_0 + \Delta t_0) = \frac{a(t_0 + \Delta t_0)}{a(t_{\rm em} + \Delta t_{\rm em})} - 1\,, \tag{2}$$

where $\Delta t_{\rm em}$ is the scale representing the time interval when the source emitted the other signal. It should satisfy $\Delta t_{\rm em} = \Delta t_0/(1 + z)$. The observed change in redshift of the source is thus given by

$$\Delta z = \frac{a(t_0 + \Delta t_0)}{a(t_{\rm em} + \Delta t_{\rm em})} - \frac{a(t_0)}{a(t_{\rm em})}\,. \tag{3}$$

A further relation can be obtained if we keep the first order approximation

$$\Delta z \approx \left[\frac{\dot{a}(t_0) - \dot{a}(t_{\rm em})}{a(t_{\rm em})}\right] \Delta t_0\,. \tag{4}$$

Clearly, the observable Δz is a direct change in the expansion rate during the evolution of the universe. In terms of the Hubble parameter $H(z) = \dot{a}(t_{\rm em})/a(t_{\rm em})$, it can be simplified as

$$\frac{\Delta z}{\Delta t_0} = (1 + z)H_0 - H(z)\,. \tag{5}$$

This is also well known as the McVittie Equation (McVittie 1962). Obviously, redshift drift is associated with cosmological models through the Hubble parameter $H(z)$.

Figure 1 shows the theoretical redshift drift for different standard cosmological models. We find that redshift drift at low redshift generally tends towards negative behavior with the predominance of

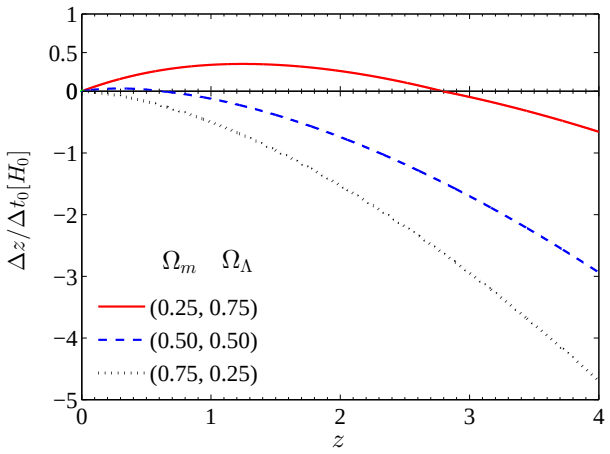

Fig. 1 Redshift drift in different standard cosmological models with space being flat.

the dark matter parameter Ω_m. This feature is often regarded as a means to distinguish dark energy models from Lemaitre-Tolman-Bondi models at $z < 2$ (especially at low redshift) (Yoo et al. 2011). Unfortunately however, CODEX would not be able to measure this drift at low z, since the Lyα forest can be measured from the ground only at $z \geq 1.7$ (Liske et al. 2008a). Therefore, acquisition of Δz at low z is required. Moreover, elimination of redshift drift ($\Delta z = 0$) at a certain redshift is also our intention. It is usually expected to occur at $z \approx 2$. Observationally, this change in redshift can also be expressed as a spectroscopic velocity drift

$$\frac{\Delta v}{\Delta t_0} = \frac{c}{1+z}\frac{\Delta z}{\Delta t_0}\,. \tag{6}$$

It can usually be detected at an order of several cm s^{-1} yr^{-1}.

In the field of cosmology research, a criterion of acceleration is the deceleration factor $q(z) \equiv -\ddot{a}/(aH^2(z))$. Through a series of calculations, we derive the following equation

$$\begin{aligned} q(z) &= \frac{1}{E(z)}\frac{dE(z)}{dz}(1+z) - 1 \\ &= \frac{1 - \left(\frac{\Delta z}{\Delta t_0}\right)'}{1 - \frac{1}{1+z}\frac{\Delta z}{\Delta t_0}} - 1\,, \end{aligned} \tag{7}$$

where the prime denotes derivative with respect to z. In the calculation, redshift drift is in units of H_0. We find that the deceleration factor not only depends on the redshift drift Δz, but is also related to its slope $(\Delta z)'$. Considering Equation (5), we obtain the slope

$$\left(\frac{\Delta z}{\Delta t_0}\right)' = H_0\big[1 - E'(z)\big]\,, \tag{8}$$

where $E(z) \equiv H(z)/H_0$ is the dimensionless expansion rate. Obviously, the slope is positive for $E'(z) < 1$ and negative for $E'(z) > 1$. For a standard cosmological model, the expansion rate $\dot{a}(z)$ behaves like a quadratic curve. We investigate the relation between deceleration factor and redshift drift, and find that the former focuses on the rate of change $\dot{a}(z)$, while the latter concentrates on the variation of $\dot{a}(z)$ during the time interval for observations Δt_0. In the period of decelerating

expansion, the redshift drift changes from negative to positive. The location of the transition changes in different cosmological models. In the period of accelerated expansion, redshift drift is always positive.

In the following section, we will focus our attention on reconstructing the velocity drift and the deceleration factor using some current observational data. We also perform some comparisons with the simulated data from Liske et al. (2008a,b, 2009).

3 REDSHIFT DRIFT CONSTRUCTION

3.1 Observational Data

To derive a better constraint on cosmological parameters, one often makes a joint analysis with different combinations of observational data sets. Recently, Su et al. (2011) found that the combination of SNeIa, shift parameter R based on CMB data, distance parameter A based on BAO data, and observational $H(z)$ data (OHD) is a better choice using the criterion which estimates the constraining power of cosmological data. In this paper, we adopt this scheme.

3.1.1 Hubble parameter

The available OHD are found through differential ages of galaxies (Jimenez & Loeb 2002; Simon et al. 2005; Stern et al. 2010) and the BAO peaks (Gaztañaga et al. 2009; Moresco et al. 2012). Data used in this paper are listed in table 2 of Zhang et al. (2012), which incorporates 21 published values of $H(z)$ with associated errors.

Using the OHD, best-fitting values of the parameters are determined by minimizing the formula

$$\chi^2_{\rm OHD}(H_0, z, \boldsymbol{p}) = \sum_i \frac{[H_0 E(z_i) - H^{\rm obs}(z_i)]^2}{\sigma_i^2}\,, \tag{9}$$

where $\boldsymbol{p}$ stands for the parameter vector of each dark energy model and $H^{\rm obs}$ represents the observational data. In the calculation, we use $H_0 = 74.3 \pm 2.1$ km s^{-1} Mpc^{-1} (Freedman et al. 2012) as the prior from the calibration of Cepheids published by the *Carnegie Hubble Program*.

3.1.2 Luminosity distance

Owing to their rich abundance of data, SNeIa are another widely used tool. In this paper, we will use the latest sample, the Union2.1 data set (Suzuki et al. 2012), which contains 580 SNeIa. They are usually presented as tabulated distance moduli with errors. Physically, the difference between the apparent magnitude m and the absolute magnitude M is estimated through

$$\mu_{\rm th}(z) = m(z) - M = 5\log_{10} D_L(z) + \mu_0\,, \tag{10}$$

where $\mu_0 = 42.38 - 5\log_{10} h$, and h is the Hubble constant H_0 in units of 100 km s^{-1} Mpc^{-1}. The corresponding luminosity distance function $D_L(z)$ can be expressed as

$$D_L(z) = \frac{1+z}{\sqrt{|\Omega_k|}}\,{\rm sinn}\left[\sqrt{|\Omega_k|}\int_0^z \frac{{\rm d}z'}{E(z';\boldsymbol{p})}\right]\,, \tag{11}$$

where the sinn function is defined by

$${\rm sinn}(x) = \begin{cases} \sinh x\,, & \Omega_k > 0\,, \\ x\,, & \Omega_k = 0\,, \\ \sin x\,, & \Omega_k < 0\,. \end{cases} \tag{12}$$

In this definition, the dimensionless Hubble parameter $E(z';\boldsymbol{p})$ is independent of the parameter h. The parameters in theoretical models are determined by minimizing the expression

$$\chi^2_{\rm SN}(H_0, z, \boldsymbol{p}) = \sum_i \frac{[\mu_{\rm obs}(z) - \mu_{\rm th}(z)]^2}{\sigma_i^2(z)}\,, \tag{13}$$

where $\mu_{\rm obs}$ represents the observed distance moduli and σ_i is the uncertainty in the distance moduli given by the data. The expression for the theoretical distance moduli $\mu_{\rm th}$ is defined in Equation (10). Generally, the nuisance parameter μ_0 can be marginalized. However, an alternative way can be carried out following previous work (Nesseris & Perivolaropoulos 2005; Perivolaropoulos 2005; di Pietro & Claeskens 2003). The χ^2 of Equation (13) with respect to μ_0 can eventually be transformed into a modified expression (Su et al. 2011)

$$\tilde{\chi}^2_{\rm SN}(z, \boldsymbol{p}) = A - \frac{B^2}{C}\,, \tag{14}$$

where

$$\begin{aligned} A(\boldsymbol{p}) &= \sum_i \frac{[\mu_{\rm obs}(z) - \mu_{\rm th}(z;\mu_0 = 0, \boldsymbol{p})]^2}{\sigma_i^2(z)}, \\ B(\boldsymbol{p}) &= \sum_i \frac{\mu_{\rm obs}(z) - \mu_{\rm th}(z;\mu_0 = 0, \boldsymbol{p})}{\sigma_i^2(z)}, \\ C &= \sum_i \frac{1}{\sigma_i^2(z)}\,. \end{aligned} \tag{15}$$

Due to the equivalence between Equations (13) and (14), we can instead minimize $\tilde{\chi}^2_{\rm SN}$ to obtain the best-fit parameters. This approach has commonly been used in calculations of the parameter constraint (Wei 2010), reconstruction of dark energy (Wei et al. 2007), etc.

3.1.3 Cosmic microwave background

Besides SNeIa, shift parameter R, obtained from acoustic oscillations in the CMB temperature anisotropy power spectrum (Hinshaw et al. 2009; Komatsu et al. 2009), is also widely used to constrain cosmological models. The complete expression is

$$R = \frac{\sqrt{|\Omega_m|}}{\sqrt{|\Omega_k|}}\,\mathrm{sinn}\left[\sqrt{|\Omega_k|}\int_0^{z_s}\frac{\mathrm{d}z'}{E(z';\boldsymbol{p})}\right], \tag{16}$$

where $z_s = 1091.3$ is the redshift of recombination (Hu & Sugiyama 1996). The observational value of R is adopted from WMAP7 (Komatsu et al. 2011). In this case the corresponding χ^2 is defined as

$$\chi^2_R = \left(\frac{R - 1.725}{0.018}\right)^2. \tag{17}$$

3.1.4 Baryon acoustic oscillation

The distance parameter A is another effective constraint on parameters. It is the measurement of the BAO peak in the distribution of SDSS luminous red galaxies (Eisenstein et al. 2005). Its form is (Guo et al. 2006)

$$A = \frac{\sqrt{\Omega_m}}{z_1}\left\{\frac{z_1}{E(z_1)}\frac{1}{|\Omega_k|}\,\mathrm{sinn}^2\left[\sqrt{|\Omega_k|}\int_0^{z_1}\frac{\mathrm{d}z'}{E(z';\boldsymbol{p})}\right]\right\}^{1/3}, \tag{18}$$

where $z_1 = 0.35$. The corresponding χ^2 suggested by WMAP7 is as follows

$$\chi^2_{\rm A} = \left(\frac{A - 0.472}{0.017}\right)^2 . \tag{19}$$

With these definitions, the parameters in theoretical models are determined from the total χ^2

$$\chi^2 = \chi^2_{\rm OHD} + \tilde{\chi}^2_{\rm SN} + \chi^2_{\rm R} + \chi^2_{\rm A} . \tag{20}$$

This group can generally also be found in analyzing the criterion of observational data (Su et al. 2011), model parameterizations (Lazkoz & Majerotto 2007) and other related work.

3.2 Construction Scheme

Undetermined parameters in $\boldsymbol{p}$ for models and their errors at different confidence levels can be estimated by the joint constraints from observational data. With the estimation of parameters in $\boldsymbol{p}$, the objective function F can be reconstructed by error propagation. In this paper, we adopt the method proposed by Lazkoz et al. (2012). Generally, joint constraints can provide an estimation of the ith parameter $p_i = p_{0i}{}^{+\sigma_{i\rm u}}_{-\sigma_{i\rm l}}$, where p_{0i} is the best-fit value, and $\sigma_{i\rm u}$, and $\sigma_{i\rm l}$ are the upper bound and lower bound, respectively. For sufficiently small errors, errors of the objective function F are therefore estimated by

$$\begin{aligned} \delta F_{\rm u} &= \sqrt{\sum_i \left[\max\left(\frac{\partial F}{\partial p_i}\sigma_{i\rm u}, -\frac{\partial F}{\partial p_i}\sigma_{i\rm l}\right)\right]^2}, \\ \delta F_{\rm l} &= \sqrt{\sum_i \left[\min\left(\frac{\partial F}{\partial p_i}\sigma_{i\rm u}, -\frac{\partial F}{\partial p_i}\sigma_{i\rm l}\right)\right]^2}, \end{aligned} \tag{21}$$

where $\delta F_{\rm u}$ and $\delta F_{\rm l}$ are its upper limit and lower limit, respectively. In Gaussian situations, the estimations above finally reduce to the standard error propagation formula $\delta F_{\rm u} = \delta F_{\rm l}$. The objective function F considered in our paper incorperates the velocity drift and the deceleration factor. What deserves special mention is that the objective function F in Equation (21) is a general form of the reconstructed parameter. In the present paper, the function F should be interpreted as the velocity drift Δv and the deceleration factor $q(z)$ that we will reconstruct in following sections. Therefore, errors of the reconstructed Δv and $q(z)$ can be calculated according to Equation (21).

4 RESULTS IN DIFFERENT COSMOLOGICAL MODELS

The number of proposed candidates for dark energy is huge. For simplification, we mainly perform analysis in the present paper on four common models, the ΛCDM model, XCDM model, CPL model and Dvali-Gabadadze-Porrati (DGP) model.

4.1 ΛCDM Model

The simplest model for dark energy is the ΛCDM model, which states that the cosmological constant is the impetus of the accelerating expansion. The Hubble parameter in such a model is given by

$$E^2(z) = \Omega_m(1+z)^3 + \Omega_k(1+z)^2 + \Omega_\Lambda . \tag{22}$$

Using the normalization condition on space curvature $\Omega_k = 1 - \Omega_m - \Omega_\Lambda$, two free parameters are determined from the joint constraints formulated in Equation (20). By minimizing the total χ^2,

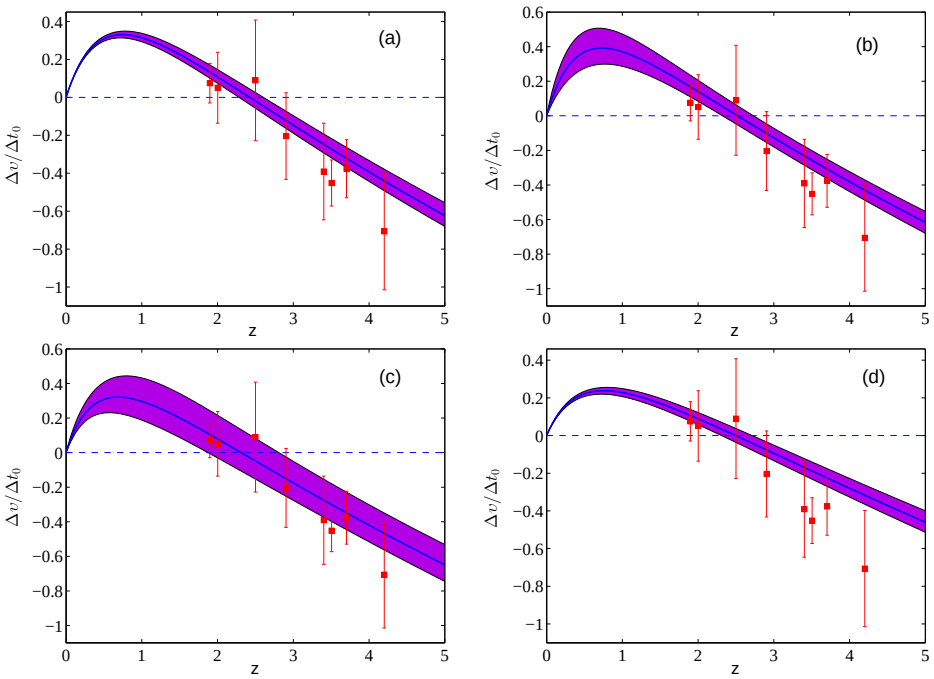

Fig. 2 Reconstruction of velocity drift for different cosmological models. (a) ΛCDM; (b) XCDM; (c) CPL; (d) DGP. The shaded regions are reconstructed results from observational data with 1σ. The solid curves in regions are the best-fit velocity drift. Eight points with errorbars are simulated velocity drift data from Liske et al. (2008a,b, 2009), which are in units of cm s^{-1} yr^{-1}.

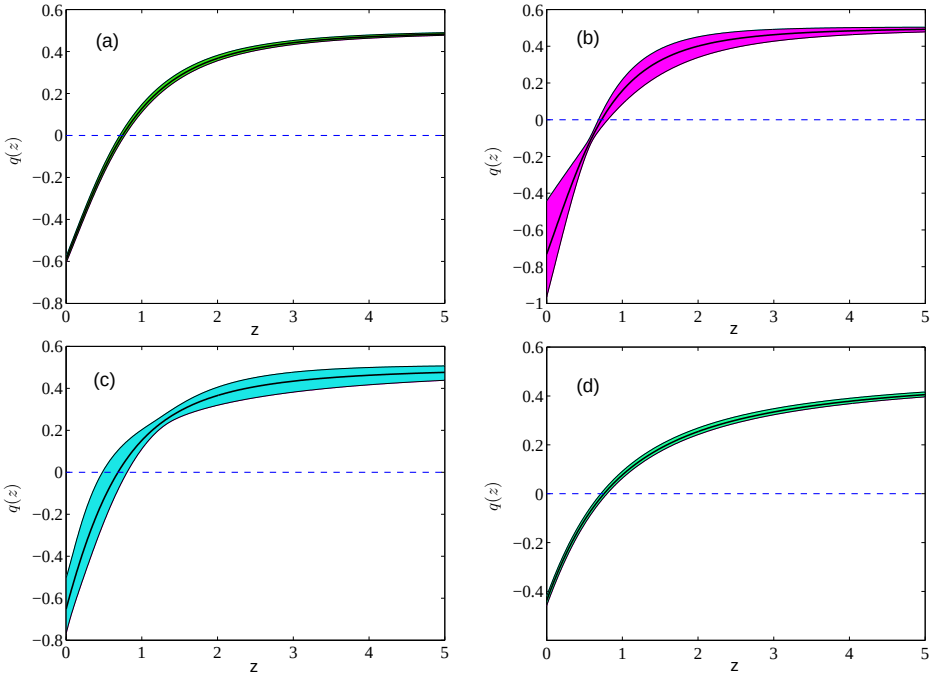

Fig. 3 Reconstruction of the deceleration factor for different cosmological models. (a) ΛCDM; (b) XCDM; (c) CPL; (d) DGP.

we obtain the matter component $\Omega_m = 0.2750^{+0.0164}_{-0.0133}$ and dark energy $\Omega_\Lambda = 0.7290^{+0.0113}_{-0.0136}$ with $\chi^2_{\rm min}$ =584.5358. With estimation of the parameters, we can respectively reconstruct the velocity drift and deceleration factor by performing the method described by Equation (21). The velocity drift profile is shown in the top left of Figure 2. We find it increases with the decrease of redshift, and turns down at $z = 0.78$ with a peak value of 0.35. Within a 1σ confidence level, the result indicates that transition from $\Delta z > 0$ to $\Delta z < 0$ happens at redshift in the range [2.28, 2.61], which, among these models, is the earliest to arrive at the transition point. We also compare the result with the simulated data. We find that the ΛCDM model agrees the best with the simulated data.

For further study, we also reconstruct the deceleration factor in Figure 3. We find that the transition from deceleration to acceleration happens at approximately redshift $z = 0.75$. The current deceleration factor is estimated to be $q_0 = -0.6$ which acts as a small error in the standard cosmological model.

4.2 XCDM Model

Specializing to a non-flat Friedmann-Robertson-Walker universe, the expansion rate with a constant EoS w is given by

$$E^2(z) = \Omega_m(1+z)^3 + \Omega_k(1+z)^2 + \Omega_\Lambda(1+z)^{3(1+w)}\,. \tag{23}$$

The dark energy models can be distinguished by their different EoSs. In addition to the case where cosmological constant $w = -1$, this class of models also includes quiessence with $-1 < w < 0$, quintessence with $-1 < w < 1$, and phantom with $w < -1$. Joint constraints give dark matter density parameter $\Omega_m = 0.2760^{+0.0145}_{-0.0149}$, dark energy parameter $\Omega_\Lambda = 0.7325^{+0.0130}_{-0.0136}$ and $w = -1.125^{+0.2115}_{-0.2627}$ with $\chi^2_{\rm min}$ =583.4215. Estimation of the fitted EoS suggests that the dark energy behaves like a phantom at the 1σ level.

Reconstruction of velocity drift in the top right panel of Figure 2 shows a peak value of 0.5, which is maximal among these models. The result with the 1σ confidence level indicates a transition occurs in the range [2.32, 2.72], which is slightly later than that in the standard model. When compared with the simulated data, a better agreement with the standard model is obtained. Reconstruction of the deceleration factor in Figure 3 provides the same transition as the ΛCDM model but with a bigger error estimation at low redshift. To a degree, constant w over the whole redshift space may be unsuitable for explaining the observational data.

4.3 CPL Model

Besides dark energy models with constant EoS, more dynamical models have been proposed. If the EoS of dark energy is time dependent, the corresponding equation for the rate of expansion is

$$E^2(z) = \Omega_m(1+z)^3 + \Omega_k(1+z)^2 + \Omega_\Lambda \exp\left[3\int_0^z \frac{1+w(z)}{1+z}dz\right]\,. \tag{24}$$

The most commonly used form of EoS is the CPL parametrization $w = w_0 + w_1 z/(1+z)$ (Chevallier & Polarski 2001; Linder 2003). According to the joint analysis, the parameters are listed as: dark matter $\Omega_m = 0.2774^{+0.0227}_{-0.0184}$, dark energy $\Omega_\Lambda = 0.7250^{+0.0114}_{-0.0161}$, $w_0 = -1.06^{+0.1350}_{-0.1062}$ and $w_1 = 0.3^{+0.6608}_{-0.8335}$ with a moderate $\chi^2_{\rm min}$ =584.2995. Although the current EoS w_0 approaches the cosmological constant, rate of change w_1 significantly deviates from zero.

With these estimations, the velocity drift is also reconstructed. Its error is bigger than those of the above models in the whole region. The transition is estimated to occur at redshift in the range [1.87, 2.8]. By comparing the reconstructed Δv with the simulated data, we find that the former is

consistent with the latter. The reconstructed Δv within 1σ confidence level is mainly in the region allowed by the simulated data. Moreover, the reconstructed deceleration factor shows that q_0 is in [–0.8 –0.5], which is a wider range than the ΛCDM model but narrower than the XCDM model.

4.4 DGP Model

The DGP brane world model (Dvali et al. 2000) is a well-known modification to general relativity for the accelerated explanation. Unlike other theories, the DGP model arises from the brane world theory in which gravity leaks out into the bulk at large scales, which eventually leads to the possibility of an accelerated expansion of the universe (Guo et al. 2006). In such a model, the rate of expansion is determined by

$$E^2(z) = \Omega_k(1+z)^2 + \left[\sqrt{\Omega_{r_c}} + \sqrt{\Omega_{r_c} + \Omega_m(1+z)^3}\right]^2 , \tag{25}$$

where the subscript r_c is the crossover scale beyond which the gravitational force follows the five-dimensional $1/r^3$ behavior. The bulk-induced term Ω_{r_c} is defined as

$$\Omega_{r_c} \equiv \frac{1}{4r_c^2 H_0^2} . \tag{26}$$

The joint constraint from observational data shows a slightly smaller dark matter density parameter $\Omega_m = 0.2142^{+0.0143}_{-0.0121}$ than other models. Furthermore, the bulk-induced density parameter $\Omega_{rc} = 0.1455^{+0.0041}_{-0.0050}$ is obviously less than the dark energy density in other models and has a crude $\chi^2_{\rm min} = 612.5485$.

The bottom right panel of Figure 2 shows a slender profile of the velocity drift for the DGP model. The result has a peak value of 0.25, which is the smallest among these models. It is worth stating that the profile appears to be quite similar to that of the standard cosmological model at redshift $z \lesssim 3$ when compared with the simulated velocity drift. However, it is obviously inconsistent with the data towards higher redshift. Estimation of today's deceleration factor q_0 is about –0.5 with a very small error.

5 CONCLUSIONS AND DISCUSSION

In this paper, motivated by interest in the redshift drift, we reconstruct the velocity drift and deceleration factor using some observational data. The data used here are respectively observational $H(z)$ data from the differential ages of galaxies and BAO peaks, luminosity distances from the Union2.1 sample of SNeIa, shift parameter R from WMAP7 and BAO distance parameter A from SDSS.

Velocity drifts are reconstructed for the standard cosmological model, XCDM model, CPL model and DGP model. They are shown in Figure 2. We find that they give a similar profile but with different peak values. The difference among peak values may provide a potential test of various cosmological models. We also investigate the transition of velocity drift from negative to positive at the 1σ confidence level. Estimations are different from each other. For the standard model, it occurs at $z < 2.61$. When compared with the simulated velocity drift from Liske et al. (2008a,b, 2009), we find that the DGP model behaves similarly to the standard model at redshift $z \lesssim 3$, but deviates from the simulation at higher redshift.

Figure 2 shows that behaviors of the reconstructed velocity drift are similar at high redshift. However, they can be distinguished at low redshift with different peak values and different corresponding redshift. Therefore, detection at low redshift is required. This is also demonstrated by Moraes & Polarski (2011) from the comparison between SNeIa and redshift drift for oscillating dark energy models. Unfortunately, redshift drifts at low redshift ($z = 0.09 - 0.69$) measured by Darling (2012) from the precise HI 21 cm absorption line primarily using the Green Bank Telescope are

about three orders of magnitude larger than the theoretically expected values. Therefore, improving the long-term stability in frequency or developing a new scheme are feasible directions for this work.

An important criterion of the expansion history of the universe is the deceleration factor $q(z)$, an instantaneous estimation of the expansion at cosmic time. The transition from decelerating expansion to accelerating expansion is most important. Investigations of it with different observations have been controversial. For example, the latest estimation from a list of 28 independent measurements of OHD is $z_{\rm da} = 0.74 \pm 0.05$ (Farooq & Ratra 2013), but evaluation from SNeIa provides a lower transition at $z_{\rm t} = 0.60^{+0.28}_{-0.11}$ (Cunha & Lima 2008). Our reconstructions of $q(z)$ are shown in Figure 3. Joint constraints on the transition generally happen at redshift $z_{\rm t} \sim 0.7$, which agrees well with estimation from only using OHD (Farooq & Ratra 2013). Furthermore, our results demonstrate that the deceleration factor now generally has a value of $q_0 \sim -0.6$ except in the DGP model.

Although our reconstructions are restricted to specific models, they provide an objective and quantified understanding of the redshift drift for the first time. Our results reveal the importance of the redshift drift, especially at low redshifts. Different peak values and corresponding redshifts provide insight on this issue. Moreover, transition of $q(z)$ is usually estimated using a single data set. However, reconstructions in this paper are based on the joint constraints. Certainly, our results, by contrast, provide a more complete estimation. On the other hand, quantitative evaluation on the power of redshift drift and the relation between $q(z)$ and Δz will also be investigated in our future work.

Acknowledgements M. J. Zhang would like to thank Zhong-Xu Zhai for a valuable discussion, and to thank Shuo Yuan, De-Zi Liu and Shuo Cao for their kind help on some related calculations. We would also like to thank Dr. Joe Liske and Bruno Moraes for the discussion of redshift drift and the deceleration factor. This work was supported by the National Natural Science Foundation of China (Grant Nos.11235003, 11175019 and 11178007).

References

Armendariz-Picon, C., Mukhanov, V., & Steinhardt, P. J. 2000, Physical Review Letters, 85, 4438
Balbi, A., & Quercellini, C. 2007, MNRAS, 382, 1623
Caldwell, R. R., Kamionkowski, M., & Weinberg, N. N. 2003, Physical Review Letters, 91, 071301
Chevallier, M., & Polarski, D. 2001, International Journal of Modern Physics D, 10, 213
Cunha, J. V. 2009, Phys. Rev. D, 79, 047301
Cunha, J. V., & Lima, J. A. S. 2008, MNRAS, 390, 210
Darling, J. 2012, ApJ, 761, L26
di Pietro, E., & Claeskens, J.-F. 2003, MNRAS, 341, 1299
Dvali, G., Gabadadze, G., & Porrati, M. 2000, Physics Letters B, 485, 208
Eisenstein, D. J., Zehavi, I., Hogg, D. W., et al. 2005, ApJ, 633, 560
Farooq, O., & Ratra, B. 2013, ApJ, 766, L7
Feng, B., Wang, X., & Zhang, X. 2005, Physics Letters B, 607, 35
Freedman, W. L., Madore, B. F., Scowcroft, V., et al. 2012, ApJ, 758, 24
Gaztañaga, E., Cabré, A., & Hui, L. 2009, MNRAS, 399, 1663
Guo, Z.-K., Zhu, Z.-H., Alcaniz, J. S., & Zhang, Y.-Z. 2006, ApJ, 646, 1
Hinshaw, G., Weiland, J. L., Hill, R. S., et al. 2009, ApJS, 180, 225
Hu, W., & Sugiyama, N. 1996, ApJ, 471, 542
Jain, D., & Jhingan, S. 2010, Physics Letters B, 692, 219
Jimenez, R., & Loeb, A. 2002, ApJ, 573, 37
Komatsu, E., Dunkley, J., Nolta, M. R., et al. 2009, ApJS, 180, 330
Komatsu, E., Smith, K. M., Dunkley, J., et al. 2011, ApJS, 192, 18
Lazkoz, R., & Majerotto, E. 2007, J. Cosmol. Astropart. Phys., 7, 015

Lazkoz, R., Montiel, A., & Salzano, V. 2012, Phys. Rev. D, 86, 103535
Linder, E. V. 2003, Physical Review Letters, 90, 091301
Liske, J., Grazian, A., Vanzella, E., et al. 2008a, MNRAS, 386, 1192
Liske, J., Grazian, A., Vanzella, E., et al. 2008b, The Messenger, 133, 10
Liske, J., Pasquini, L., Bonifacio, P., et al. 2009, in Science with the VLT in the ELT Era, ed., A. Moorwood, 243
Loeb, A. 1998, ApJ, 499, L111
Maor, I., Brustein, R., & Steinhardt, P. J. 2001, Physical Review Letters, 86, 6
McVittie, G. C. 1962, ApJ, 136, 334
Moraes, B., & Polarski, D. 2011, Phys. Rev. D, 84, 104003
Moresco, M., Cimatti, A., Jimenez, R., et al. 2012, J. Cosmol. Astropart. Phys., 8, 006
Nesseris, S., & Perivolaropoulos, L. 2005, Phys. Rev. D, 72, 123519
Nojiri, S., & Odintsov, S. D. 2007, International Journal of Geometric Methods in Modern Physics, 4, 115
Padmanabhan, T., & Choudhury, T. R. 2002, Phys. Rev. D, 66, 081301
Pasquini, L., Cristiani, S., Dekker, H., et al. 2005, The Messenger, 122, 10
Pasquini, L., Cristiani, S., Dekker, H., et al. 2006, in IAU Symposium, 232, The Scientific Requirements for Extremely Large Telescopes, eds. P. Whitelock, M. Dennefeld, & B. Leibundgut, 193
Peebles, P. J. E., & Ratra, B. 1988, ApJ, 325, L17
Perivolaropoulos, L. 2005, Phys. Rev. D, 71, 063503
Piazza, F., & Tsujikawa, S. 2004, J. Cosmol. Astropart. Phys., 7, 004
Planck Collaboration, Ade, P. A. R., Aghanim, N., et al. 2013, arXiv:1303.5076
Riess, A. G., Filippenko, A. V., Challis, P., et al. 1998, AJ, 116, 1009
Sandage, A. 1962, ApJ, 136, 319
Simon, J., Verde, L., & Jimenez, R. 2005, Phys. Rev. D, 71, 123001
Spergel, D. N., Verde, L., Peiris, H. V., et al. 2003, ApJS, 148, 175
Stern, D., Jimenez, R., Verde, L., Kamionkowski, M., & Stanford, S. A. 2010, J. Cosmol. Astropart. Phys., 2, 008
Su, Q., Tuo, Z.-L., & Cai, R.-G. 2011, Phys. Rev. D, 84, 103519
Suzuki, N., Rubin, D., Lidman, C., et al. 2012, ApJ, 746, 85
Tegmark, M., Strauss, M. A., Blanton, M. R., et al. 2004, Phys. Rev. D, 69, 103501
Uzan, J.-P., Clarkson, C., & Ellis, G. F. R. 2008, Physical Review Letters, 100, 191303
Wei, H. 2010, J. Cosmol. Astropart. Phys., 8, 020
Wei, H., Tang, N., & Zhang, S. N. 2007, Phys. Rev. D, 75, 043009
Wright, E. L. 2007, ApJ, 664, 633
Yoo, C.-M., Kai, T., & Nakao, K.-I. 2011, Phys. Rev. D, 83, 043527
Zhang, C., Zhang, H., Yuan, S., Zhang, T.-J., & Sun, Y.-C. 2012, arXiv:1207.4541
Zhang, H., Zhong, W., Zhu, Z.-H., & He, S. 2007, Phys. Rev. D, 76, 123508
Zhang, J., Zhang, L., & Zhang, X. 2010, Physics Letters B, 691, 11